Reduction of The Pyruvate Decarboxylase Activity Improves Isobutanol Production By *Klebsiella Pneumoniae*

Lin Shu
Shanghai Advanced Research Institute Chinese Academy of Sciences: Chinese Academy of Sciences Shanghai Advanced Research Institute
Jinjie Gu
Shanghai Advanced Research Institute Chinese Academy of Sciences: Chinese Academy of Sciences Shanghai Advanced Research Institute
Qinghui Wang
Shanghai Advanced Research Institute Chinese Academy of Sciences: Chinese Academy of Sciences Shanghai Advanced Research Institute
Shaoqi Sun
Shanghai Advanced Research Institute Chinese Academy of Sciences: Chinese Academy of Sciences Shanghai Advanced Research Institute
Youtian Cui
University of California Davis
Jason Fell
University of California Davis
Wai Shun Mak
University of California Davis
Justin B. Siegel
University of California Davis
Jiping Shi
Shanghai Advanced Research Institute Chinese Academy of Sciences: Chinese Academy of Sciences Shanghai Advanced Research Institute
Gary J. Lye
University College London
Frank Baganz
University College London
Jian Hao (haoj@sari.ac.cn)
Shanghai Advanced Research institute, CAS https://orcid.org/0000-0002-4403-8188

Research

Keywords: Isobutanol, 2-Ketoisovalerate decarboxylase, Indole-3-pyruvate decarboxylase, Klebsiella pneumoniae

Posted Date: December 14th, 2021

DOI: https://doi.org/10.21203/rs.3.rs-1155955/v1

Abstract

Background

Klebsiella pneumoniae contains an endogenous isobutanol synthesis pathway. *ipdC*, annotated as an indole-3-pyruvate decarboxylase (Kp-IpdC), was identified to catalyze the formation of isobutyraldehyde from 2-ketoisovalerate.

Results

Compared with 2-ketoisovalerate decarboxylase from *Lactococcus lactis* (KivD), a decarboxylase commonly used in artificial isobutanol synthesis, Kp-IpdC has an 2.8-fold lower K_m for 2-ketoisovalerate, leading to higher isobutanol production without induction. However, high level expression of *ipdC* by induction resulted in a low isobutanol titer. *In vitro* enzymatic reactions showed that Kp-IpdC exhibits promiscuous pyruvate decarboxylase activity, which adversely consume the available pyruvate precursor for isobutanol synthesis. To address this we have engineered Kp-IpdC to reduce pyruvate decarboxylase activity. From computational modeling we identified 10 residues surrounding the active site for mutagenesis. Ten designs consisting of eight single-point mutants and two double-mutants were selected for exploration. Mutants L546W and T290L showed 5.1% and 22.1% of catalytic efficiency on pyruvate, which were then expressed in *K. pneumoniae* for *in vivo* test. Isobutanol production by *K. pneumoniae* T290L was 25% higher than the control strain, and a final titer of 5.5 g/L isobutanol was obtained with a substrate conversion ratio of 0.16 mol/mol glucose.

Conclusions

This research provides a new way to improve the efficiency of the biological route of isobutanol production.

Highlights

1. Kp-IpdC is more efficient than KivD in 2-ketoisovalerate decarboxylation

2. Pyruvate decarboxylase activity is a limitation of Kp-IpdC

3. T290L variant holds a decreased pyruvate decarboxylase activity

4. Isobutanol production by K. pneumoniae T290L was improved

Background

Production of sustainable bioenergy for industrial usage has been a very important capability in biotechnology. This technology tries to find solutions for today's globally significant ecological and energy challenges, including the high rate of climate change and increased consumption of fossil fuels [1]. The primary biofuel for the gasoline market has historically been ethanol manufactured from corn. However, a number of drawbacks have been identified with ethanol use: it has a lower energy content compared to gasoline, it is not amenable to pipeline distribution, and the amount that can be blended into gasoline for use in conventional vehicles is limited by environmental regulations and engine compatibility [2]. Higher molecular weight alcohols such as n-butanol and isobutanol have higher energy contents and should be more amenable to pipeline distribution [3]. Isobutanol can be blended with diesel and biodiesel in high ratios [4]. Compared to diesel fuel, CO and NOx emissions decrease with the use of blends of isobutanol and diesel [5]. Isobutanol is also used as a precursor in lubricants, coatings, adhesives, car paint sprays, and the pharmaceutical industry.

Isobutanol is a component of fusel oil (15%), the latter is a by-product of the bioethanol industry [6]. *Saccharomyces cerevisiae* is the only known natural microorganism that can synthesize isobutanol at a detectable level. Isobutanol and other components of the fusel oil can be synthesized from amino acids via an Ehrlich pathway. Isobutanol can be also *de novo* synthesized from pyruvate. First, pyruvate is imported into mitochondria and two molecules are condensed to acetolactate by acetolactate synthase. In the subsequent step, acetolactate is reduced to 2,3-dihydroxyisovalerate by acetohydroxyacid reductoisomerase. Finally, 2,3-dihydroxyisovalerate is converted to 2-ketoisovalerate by dihydroxyacid dehydratase. 2-ketoisovalerate must then be transported into the cytosol to form isobutyraldehyde and further to isobutanol [7]. Many metabolic engineering works have been done to improve the formation of isobutanol, and 2.06 g/L of isobutanol was yielded by an *S. cerevisiae* strain by blocking competing metabolic pathways [8]. However, the main metabolite produced by *S. cerevisiae* is still ethanol.

With the development of synthetic biology, an artificial isobutanol synthesis pathway was established in *Escherichia coli* in 2008 [9]. This artificial isobutanol synthesis pathway was similar to that of *S. cerevisiae*. α-acetolactate synthase from *Bacillus subtilis*, acetohydroxyacid reductoisomerase and dihydroxyacid dehydratase from *E. coli*, 2-ketoisovalerate decarboxylase and alcohol dehydrogenase from *Lactococcus lactis* were used to catalyze the reactions in the synthesis pathway [10]. Following this strategy, the isobutanol synthesis pathway was constructed in many microorganisms, and *E. coli* produced the highest isobutanol level so far. 56.5 g/L isobutanol was produced by an engineered *E. coli* that was obtained after screening a mutant library using a biosensor approach [11].

Klebsiella pneumoniae is an important industrial microorganism, it holds the advantages of fast growth rate and does not easily be contaminated by other bacteria. Wild-type *K. pneumoniae* is an efficient 1,3-propanediol and 2,3-butanediol producer [12, 13]. Engineered strains of *K. pneumoniae* have been constructed for acetoin, gluconic acid, 2-ketogluconic acid, and xylonic acid production [14-17]. A *budA* disrupted strain of *K. pneumoniae* was found to synthesize isobutanol via an endogenous pathway [18]. This endogenous isobutanol synthesis pathway consisted of the same steps as the artificial isobutanol synthesis pathway constructed in *E. coli* and other microorganisms. Of these endogenous enzymes, an

indole-3-pyruvate decarboxylase (Kp-IpdC) that is encoded by *ipdC* was identified to catalyze the isobutyraldehyde formation from 2-ketoisovalerate (Fig. 1). However, high level expression of *ipdC* resulted in a decrease of isobutanol production [18].

Indole pyruvate decarboxylases use thiamine diphosphate (ThDP) as a cofactor and require magnesium ion for catalytic activity. ThDP dependent enzymes catalyze a broad range of different reactions involving cleavage and formation of C-C bonds, which are essential in many biosynthetic pathways [19]. The decarboxylase superfamily contains more than ten families of decarboxylases, and their structures are highly conserved [20]. The structures comprise three similarly sized domains: the N-terminal domain which binds the pyrimidine (Pyr) ring of ThDP, a middle domain and the C-terminal domain which binds the diphosphate (PP) moiety. The active site is located at the interface between two monomers, with ThDP interacting with the Pyr domain of one monomer and the PP domain of the second [21].

The objective of the present study was to reveal the mechanism of the decrease of isobutanol production by high level expression of *ipdC*. Furthermore, the three-dimensional (3D) structure of Kp-IpdC was obtained by homology modeling. Site-directed mutagenesis of Kp-IpdC was carried out to improve the catalytic performance and isobutanol production by *K. pneumoniae* IpdC.

Material And Methods

Strains, plasmids, and primers

Bacterial strains and plasmids used in this study are listed in Table 1. Primers used for PCR are listed in Table S1.

Site-directed mutagenesis of Kp-IpdC and strain construction

pMD18-T-*ipdC* was digested with *EcoR I* and *BamH I* to obtain the *ipdC* fragment, and this fragment was ligated into pET28a to generate pET28a-*ipdC*. pET28a-*ipdC* was transformed into *E. coli* BL21 for protein expression. BL21/ *kivD* was constructed using the same approach as BL21/ *ipdC*.

Oligonucleotide-directed site-specific mutagenesis was carried out on expression plasmids of Kp-IpdC variants. pET28a-L546W was constructed based on pET28a-*ipdC*. Primer pair L546W-s and L546W-a were used to amplify pET28a-L546W with pET28a-*ipdC* as the template. The PCR product was transformed to *E. coli* BL21 to get BL21/L546W. Other mutants of *ipdC* expression strains were constructed using the same approach.

pDK6-L546W was constructed in the same way as pET28a-L546W with pDK6-*ipdC* replacing pET28a-*ipdC* as the template. pDK6-L546W was transformed to *K. pneumoniae* Δ*budA*-Δ*ldhA*-Δ*ipdC* to get *K. pneumoniae* L546W.

Enzymatic reaction kinetic parameters determination

BL21/*ipdC*, BL21/*kivD*, and other *E. coli* strains expressing mutants of *ipdC* were cultured for enzyme preparation. Cells lysate was prepared by sonication and purified enzyme was obtained through a His tag Ni-NTA-Sefinose Column (Sangon Biotech®) by following the protocol given by the manufacturer.

Enzyme activities of KivD, KP-IpdC, and variants of Kp-IpdC were determined by a coupled enzymatic method. The method was based on the ability of alcohol dehydrogenase, in the presence of NADH, to reduce aldehydes formed from 2-keto acid by decarboxylase. The reaction was measured spectrophotometrically by the decrease in optical density at 340 nm. Pyruvate and 2-ketoisovalerate were used as substrates respectively. The reaction mixture contained 50 mM potassium phosphate, 1 mM $MgSO_4{\cdot}7H_2O$, 0.5 mM thiamine pyrophosphate, 0.2 mM NADH, 45 U/ml alcohol dehydrogenase of *S. cerevisiae* (Sangon Biotech®). The reaction was initiated by adding the substrates. Kinetic data were fitted to the Lineweaver-Burk plot, and the parameters such as *Km*, V_{max}, and Kcat of enzymes were determined from a linear least-squares fit.

Medium and culture condition

The fermentation medium contained 100 g/L glucose, 5 g/L yeast extract, 4 g/L corn steep liquor, 5 g/L $(NH_4)_2SO_4$, 3 g/L sodium acetate, 0.4 g/L KCl and 0.1 g/L $MgSO_4$. For the seed culture, 250-mL flasks containing 50 mL of LB medium were incubated in a rotary shaker at 37 °C and 200 rpm overnight. The seed culture was inoculated into a 5-L bioreactor (BIOSTAT-A plus Sartorius) with a working volume of 3 L. The culture pH was automatically controlled at 7. The air flow rate and agitation were 2 L/min and 300 rpm respectively. The off-gas was fed through a glass condenser, which was immerged in an ice-bath, and the condensate was collected.

Analytical methods

The biomass concentration was evaluated by determination of optical density (OD 600) with a spectrophotometer.

Chemical compounds in the broth were quantified by a Shimadzu 20AVP high performance liquid chromatography system (HPLC) (Shimadzu Corp., Kyoto, Japan) equipped with a RID-10A refractive index detector and a SPD-M20A photodiode array detector. An Aminex HPX-87H column (300×7.8 mm) (Bio-Rad, USA) was used and the column temperature was set up at 65 ºC. The mobile phase was 0.005 mol/L H_2SO_4 solution at a flow rate of 0.8 ml/min.

Homology modeling of Kp-IpdC

The Rosetta software suite is an academically developed framework for protein structure prediction and design. The three-dimensional structure of Kp-IpdC was modeled with RosettaCM [24, 25]. From the NCBI database 10 homologs with ³30% sequence identity to Kp-IpdC were selected as templates to predict the structure. 3D structures of these homologous proteins have been solved empirically. A total of 10,000 structure simulations were run and the structure with the lowest Rosetta energy was chosen.

Computational Kp-lpdC redesign

RosettaDock was used to dock the substrate to Kp-lpdC and the variants of Kp-lpdC. Previous reports about decarboxylase design [26] identify10 residues (D289, T290, Q383, A387, F388, G408, V467, I471, V542, and L546) within 8 Å of the active site of Kp-lpdC for mutagenesis. These residues were substituted with one of 12 hydrophobic amino acids. The identities of amino acids at all other residues were kept constant. These variants were docked with either 2-ketoisovalerate or pyruvate as the substrate. A total of 10,000 design simulations were run, from which the 10 designs that had the most favourable Rosetta interface energy with 2-ketoisovalerate as substrate, while unfavourable Rosetta interface energy with pyruvate as substrate were selected to construct variants of Kp-lpdC.

Results

Isobutanol production by *K. pneumoniae* using Kp-lpdC or KivD as the decarboxylase

K. pneumoniae Δ*budA*-Δ*ldhA* is an isobutanol production strain constructed previously. Kp-lpdC has been identified to catalyze the reaction of isobutyraldehyde formation from 2-ketoisovalerate. KivD is an *L. lactis* decarboxylase and has been used in all artificial isobutanol synthesis pathways. *K. pneumoniae* Δ*budA*-Δ*ldhA*-*ipdC* and *K. pneumoniae* Δ*budA*-Δ*ldhA*-*kivD* were constructed to compare the difference of the two decarboxylases on isobutanol production by *K. pneumoniae*. These two strains were batch cultured in 5 L bioreactors and induced by 1 mM IPTG. The fermentation results are shown in Fig. 2.

Cell growth and glucose consumption of the two strains were comparable. Cells were quickly growing in the first 10 hours of cultivation and cell densities were kept stable in the remaining cultivation time. 80 g/L of glucose was utilised by both two strains after 30 hours of cultivation. 2.5 and 2.9 g/L of isobutanol were produced by *K. pneumoniae* Δ*budA*-Δ*ldhA*-*ipdC* and *K. pneumoniae* Δ*budA*-Δ*ldhA*-*kivD*, respectively. 2-Ketoisovalerate was found to be accumulated in the broth of the two strains with titers of 0.5 and 5.5 g/L, respectively. Ethanol generated by the two strains were 7.4 and 6.8 g/L, respectively. 4.0 and 3.4 g/L of acetic acid were produced by the two strains after 10 hours of cultivation. The acetic acid level decreased to 2.7 g/L for *K. pneumoniae* Δ*budA*-Δ*ldhA*-*kivD* but its final level was 4.9 g/L for *K. pneumoniae* Δ*budA*-Δ*ldhA*-*ipdC*. Formate produced by the two strains were 7.1 and 5.7 g/L, respectively. 2,3-Dihydroxyisovalerate accumulated to levels of 5.0 and 6.4 g/L, respectively.

To further investigate the difference of the two decarboxylases on isobutanol production, *K. pneumoniae* Δ*budA*-Δ*ldhA*-*ipdC* and *K. pneumoniae* Δ*budA*-Δ*ldhA*-*kivD* were cultured in 5 L bioreactors without induction, and fermentation results are shown in Fig. 3.

In the conditions without induction, cell growth and catabolites production of the two strains were distinctly different. 80 g/L of glucose was exhausted by *K. pneumoniae* Δ*budA*-Δ*ldhA*-*ipdC* after 27 hours of cultivation, and the highest cell density of 12.1 OD unit was achieved after 24 hours. While glucose was not exhausted by *K. pneumoniae* Δ*budA*-Δ*ldhA*-*kivD* until 35 hours of cultivation. Isobutanol produced by the two strains was 4.5 g/L and 0.6 g/L, respectively. In contrast to isobutanol, 2-

ketoisovalerate accumulated to levels of 1.0 and 11.0 for *K. pneumoniae* Δ*budA*-Δ*ldhA*-*ipdC* and *K. pneumoniae* Δ*budA*-Δ*ldhA*-*kivD*, respectively. Ethanol and acetic acid produced by *K. pneumoniae* Δ*budA*-Δ*ldhA*-*ipdC* were 6.8 g/L and 3.2 g/L, they were 6.0 g/L and 0.5 g/L for *K. pneumoniae* Δ*budA*-Δ*ldhA*-*kivD*. Formate produced by the two strains were 8.4 and 7.1 g/L, respectively. 2,3-Dihydroxyisovalerate accumulated to levels of 9.0 and 7.7 g/L, respectively.

Determination of kinetic parameters of Kp-IpdC and KivD

Comparing the results of batch culture of *K. pneumoniae* Δ*budA*-Δ*ldhA*-*ipdC* and *K. pneumoniae* Δ*budA*-Δ*ldhA*-*kivD* with and without IPTG induction it can be concluded that Kp-IpdC favors isobutanol production at a low expression level while KivD favors isobutanol production at a high expression level. Low level expression of *kivD* coincided with a high level of 2-ketoisovalerate accumulation. However, high level expression of *ipdC* does not result in a high level of 2-ketoisovalerate. Thus, high level expression of *ipdC* might constrain the metabolic flux of 2-ketoisovalerate synthesis. To clarify this hypothesis, the kinetic parameters of the two enzymes were determined *in vitro*.

Pyruvate is a central metabolite of the cell and the substrate of the first reaction of the isobutanol synthesis pathway. Indole-3-pyruvate and pyruvate are both keto acids. Thus, we suspected that pyruvate might be a substrate of Kp-IpdC. High level expression of *ipdC* can led to more pyruvate to be converted to aldehyde and further to form ethanol or acetic acid, which limited the carbon flux of isobutanol synthesis pathway. *In vitro* enzymatic reaction of 2-ketoisovalerate and pyruvate decarboxylation catalyzed by Kp-IpdC or KivD were performed. Kinetic parameters were calculated (Fig S1, S2) and results were summarized in Table 2.

Km of Kp-IpdC for 2-ketoisovalerate was 1.8 mM, while that of KivD was 4.18 mM. This indicated the affinity of Kp-IpdC to 2-ketoisovalerate was stronger than that of KivD. *K*cat value of Kp-IpdC for 2-ketoisovalerate was higher than that of KivD. This shows Kp-IpdC is more efficient than KivD in catalysis the decarboxylation of 2-ketoisovalerate to isobutyraldehyde. Moreover, the *K*cat/*K*m of Kp-IpdC for 2-ketoisovalerate was 5445.39 $M^{-1}s^{-1}$, which was more than 6 times that of KivD. Thus, Kp-IpdC is preferred in catalysis the 2-ketoisovalerate decarboxylation reaction to KivD.

Both Kp-IpdC and KivD can use pyruvate as the substrate. The *K*m of Kp-IpdC for pyruvate was lower than that of KivD. The *K*cat of Kp-IpdC for pyruvate was higher than that of KivD. Accordingly, *K*cat/*K*m of Kp-IpdC for pyruvate was about 12 times higher than that of KivD. Therefore, Kp-IpdC is more efficient in catalysis of the pyruvate decarboxylation reaction than KivD showing the same behavior as with 2-ketoisovalerate as the substrate.

Based on this kinetic analysis Kp-IpdC is favored over KivD in catalysis of 2-ketoisovalerate decarboxylation and further conversion to isobutanol. However, Kp-IpdC exhibits promiscuous pyruvate decarboxylase activity, which adversely consume the available pyruvate precursor for isobutanol synthesis. To overcome this disadvantage, the enzyme engineering method was used to improve the performance of Kp-IpdC.

Homology modeling of Kp-lpdC

The 3D structure of Kp-lpdC from *K. pneumoniae* has not been solved empirically. From the NCBI database lpdC from *Enterobacter cloacae* (Ec-lpdC – the highest sequence identity of a known structure to Kp-lpdC) was found. Ec-lpdC has a sequence identiy of 62.12% with Kp-lpdC, and is one residue shorter in sequence length. The crystal structure of Ec-lpdC has been determined at 2.65 Å resolution (PDB ID 1OVM). The crystal structures of Ec-lpdC and other 9 proteins were used as templates to predict the structure of Kp-lpdC.

The 3D structure of Kp-lpdC obtained RosettaCM with a structural comparison to Ec-lpdC are shown in Fig. 4.

Kp-lpdC structure obtained from the RosettaCM was a homo-tetramer. Two monomers interact tightly to form the dimer, and two dimers form a tetramer. Each monomer consists of three domains with an open α/β class topology: the N-terminal Pyr domain (residues 3-180), which binds the pyrimidine part of ThDP; the middle domain (residues 181-340); and the C-terminal PP domain (residues 356-551), which binds the diphosphate moiety of the cofactor per subunit. The Pyr and PP domains contain a six-stranded parallel β-sheet flanked by a number of helices, whereas the middle domain contains a six-stranded mixed β-sheet, with several helices packing against the sheet.

The Root Mean Square Deviation (RMSD) of Kp-lpdC and Ec-lpdC monomers was 1.158 by calculation of Schrodinger's protein structure alignment. Thus, the structure of Kp-lpdC and Ec-lpdC were very similar.

Computational design of Kp-lpdC

10 designed variants of Kp-lpdC where one or two residues were substituted with other hydrophobic amino acids were obtained through design simulation, with the assumption that altering the hydrophobic interaction of the active site might affect the substrate selectivity and preference. These variants all had favorable Rosetta energy with 2-ketoisovalerate as substrate while showing unfavorable Rosetta energy with pyruvate as substrate in docking simulations.

Genes encoding these variants of Kp-lpdC were constructed by site-directed mutagenesis and overexpressed in *E. coli*. Enzymes were purified from the lysate of these *E. coli* strains. Kinetic parameters of these enzymes with 2-ketoisovalerate or pyruvate as substrates were determined, and results are shown in Fig S3-S10 and summarized in Table 3.

D289L and D289L+T290L variants lost all decarboxylation activity with 2-ketoisovalerate and pyruvate respectively. F388W lost all activity to catalyze pyruvate decarboxylation, and was observered to have lower decarboxylation activity with 2-ketoisovalerate. The *K*m and *K*cat/*K*m of F388W for 2-ketoisovalerate were 16.77 mM and 172.68 $M^{-1}s^{-1}$. While those of the wild type Kp-lpdC were 1.48 mM and 5445.39 $M^{-1}s^{-1}$, (shown in Table 2). Thus, F388W was not a suitable enzyme to be used for isobutanol production.

The *K*m of A387L, V542I, A387I+F388W, Q383M, and A387L for pyruvate were all higher than that of the wild-type Kp-lpdC (4.18 mM shown in Table 2). However, the *K*m of these enzymes for 2-ketoisovalerate were also higher than that of the wild-type Kp-lpdC (1.48 mM shown in Table 2). These enzymes were all eliminated for further investigations.

Variants L546W and T290L showed lower *K*m values for 2-ketoisovalerate, 1.01 and 1.17 mM respectively, which is lower than that of the wild Kp-lpdC. The *K*m of these two variants with pyruvate were 693.27 mM and 11.27 mM, respectively. These values were much higher compared to the 3.13 mM of the wild type Kp-lpdC (shown in Table 2). The *K*cat/*K*m values of T290L and L546W with pyruvate were 40.5 $M^{-1}s^{-1}$ and 9.61 $M^{-1}s^{-1}$, respectively. These values were much lower than the value of 5445.39 $M^{-1}s^{-1}$ of the wild type Kp-lpdC (shown in Table 2).

The 3D structures of the active center of L546W and T290L docked with 2-ketoisovalerate are shown in Fig 5. The native substrate of Kp-lpdC is indole-3-pyruvate and its catalytic pocket is suitable for the native substrate. The molecule size of indole-3-pyruvate is larger than that of 2-ketoisovalerate. Thus, reducing the size of the catalytic pocket would favor 2-ketoisovalerate as a substrate. The threonine at 290 residue was mutated to leucine in T290L. The side chain of leucine is larger and more hydrophobic than that of threonine. This structure had a smaller catalytic pocket and was more suitable for 2-ketoisovalerate-ThDP-Mg^{2+} to be bound. The molecule size of pyruvate is smaller than that of 2-ketoisovalerate, the catalytic pocket of T290L might not be suitable for the compound of pyruvate-ThDP-Mg^{2+}. The leucine at 546 residue was mutated to tryptophan in L546W. The side chain of tryptophan is closer to 2-ketoisovalerate than that of leucine in the catalytic pocket. This made the compound of 2-ketoisovalerate-ThDP-Mg^{2+} more stable in the catalytic pocket. L546W and T290L have the characteristics of enhanced affinity interaction with 2-ketoisovalerate and reduced affinity with pyruvate. These two variants were selected to be used in isobutanol production.

Isobutanol production using strains with variants of Kp-lpdC

K. pneumoniae Δ*budA*-Δ*ldhA*-Δ*ipdC* was constructed to eliminate the activity of endogenous Kp-lpdC. T290L and L546W were ligated to *K. pneumoniae* expression vector pDK6 and transformed into *K. pneumoniae* Δ*budA*-Δ*ldhA*-Δ*ipdC* to construct *K. pneumoniae* Δ*budA*-Δ*ldhA*-Δ*ipdC*-T290L (T290L) and *K. pneumoniae* Δ*budA*-Δ*ldhA*-Δ*ipdC*-L546W (L546W), respectively. *K. pneumoniae* Δ*budA*-Δ*ldhA*-Δ*ipdC*-*ipdC* (lpdC) and *K. pneumoniae* Δ*budA*-Δ*ldhA*-Δ*ipdC*-*kivD* (KivD) were constructed as control strains. These three strains were cultured in 5 L bioreactors with IPTG induction, and results are shown in Fig. 6.

Cell growth and glucose consumption of these strains were similar. After 30 hours of cultivation, the 80 g/L of glucose was all utilised by these strains. Similar to *K. pneumoniae* Δ*budA*-Δ*ldhA*-*kivD*, 12.3 g/L of 2-ketoisovalerate was accumulated in the broth of *K. pneumoniae* KivD after 30 hours of cultivation. However, 2-ketoisovalerate levels were less than 1 g/L for the other three strains. Isobutanol produced by *K. pneumoniae* KivD was 1.5 g/L, which was distinctly lower than that of other strains.

Specifically, 3.9 g/L, 4.1 g/L, and 3.8 g/L of isobutanol were produced by *K. pneumoniae* IpdC, *K. pneumoniae* T290L, and *K. pneumoniae* L546W, respectively, after 28 hours of cultivation. In addition, 10.2 g/L, 7.7 g/L, and 10.1 g/L of ethanol were produced by these strains, respectively. The decrease in isobutanol and ethanol levels towards the end of the cultivation is probably due to evaporation. All strains produced acetic acid, 2,3-Dihydroxyisovalerate and formate as by-products in similar amounts.

Ethanol and acetic acid produced by *K. pneumoniae* T290L were reduced 24% and 7% compared with that of *K. pneumoniae* IpdC. This indicated the decarboxylation reaction of pyruvate was reduced in *K. pneumoniae* T290L. However, there was little increase in isobutanol production by *K. pneumoniae* T290L compared to *K. pneumoniae* IpdC.

K. pneumoniae T290L was selected for further investigation. This strain, *K. pneumoniae* KivD and *K. pneumoniae* IpdC were cultured without IPTG induction, and the results are shown in Fig. 7.

Cell growth and glucose consumption of *K. pneumoniae* IpdC were slower than that of the other two strains. 5 g/L of glucose was unused after 32 hours of cultivation. While, glucose was exhausted by other two strains, and which were similar to that of the cultivations with IPTG induction.

High level of 2-ketoisovalerate was accumulated in the broth of *K. pneumoniae* KivD after 32 hours of cultivation with a titer of 12.5 g/L. This was close to that obtained with IPTG induction. However, isobutanol produced by this strain was only 0.32 g/L compared to 1.5 g/L with induction. Acetic acid, and formate produced by *K. pneumoniae* KivD were higher than that of the other two strains, with the titers of 4.5 g/L and 9.8 g/L, respectively.

Isobutanol produced by *K. pneumoniae* IpdC and *K. pneumoniae* T290L were 4.4 and 5.5 g/L, respectively. These titres were both higher than that obtained with IPTG induction. Ethanol produced by *K. pneumoniae* IpdC was 6.9 g/L, which was lower than that obtained with IPTG induction. Whereas ethanol produced by *K. pneumoniae* T290L was 7.8 g/L, which was nearly the same as that with IPTG induction. Acetic acid produced by the two strains were all reused by the cells, with final titers of 1.7 g/L and 1.4 g/L. Acetic acid titers were all lower than that obtained with IPTG induction. In addition, both strains produced 8.7 g/L of 2,3-Dihydroxyisovalerate and 8.5 g/L and 7.3 g/L of formate were produced by *K. pneumoniae* IpdC and *K. pneumoniae* T290L, respectively.

Isobutanol production by *K. pneumoniae* T290L was improved by 24 % compared to that by *K. pneumoniae* IpdC. However, more ethanol was produced by *K. pneumoniae* T290L in comparison to *K. pneumoniae* IpdC. By contrast, acetic acid and formate produced by *K. pneumoniae* T290L were decreased compared with *K. pneumoniae* IpdC. The substrate conversion ratio of glucose to isobutanol obtained by *K. pneumoniae* T290L was 6.7% (w/w) or 0.16 mol/mol. Isobutanol production by *K. pneumoniae* IpdC with IPTG induction was lower than that obtained without IPTG induction. *K. pneumoniae* T290L cultures showed a similar tendency indicating that high level expression of T290L still lead to more pyruvate flux into by-products production.

Discussion

Kp-IpdC is more efficient than KivD in catalysis of 2-ketoisovalerate decarboxylation

K. pneumoniae has an endogenous isobutanol synthesis pathway, and the structure of this pathway was the same as artificial isobutanol synthesis pathways constructed in *E. coli* and other microorganisms [18]. A critical enzyme in the artificial isobutanol synthesis pathway is 2-keto acid decarboxylase [9], which is common in plants, yeasts, and fungi but less so in bacteria [27]. Kp-IpdC had been identified to catalyse the 2-ketoisovalerate decarboxylation reaction in *K. pneumoniae*. While all artificial isobutanol synthesis pathways reported using KivD from *L. lactis* catalyse this decarboxylation reaction [9, 28-31]. The *in vitro* experiments results shown in Table 2 indicated the efficiency of Kp-IpdC was higher than that of KivD in catalysis of 2-ketoisovalerate decarboxylation. pDK6 is a high copy vector used for protein expression in *K. pneumoniae*, this plasmid uses the tac promoter for gene expression. With IPTG induction, the protein expressed would constitute more than 1% of total cellular protein. In the absence of induction, the protein was also expressed to a certain level [22]. Kp-IpdC and KivD were all expressed in *K. pneumoniae* Δ*budA*-Δ*ldhA* without induction of IPTG. Higher level of isobutanol was obtained by *K. pneumoniae* Δ*budA*-Δ*ldhA-ipdC* than that of *K. pneumoniae* Δ*budA*-Δ*ldhA-kivD* (shown in Fig. 3) consistent with the *in vitro* experimental results. The comparison of isobutanol production by *K. pneumoniae* KivD and *K. pneumoniae* IpdC (Fig. 6, 7) showed further clear results. Thus, Kp-IpdC is more efficient than KivD in catalysis of 2-ketoisovalerate decarboxylation. If KivD was replaced by Kp-IpdC in the artificial isobutanol synthesis pathways, the isobutanol titers might potentially be significantly improved.

Catalysis Of Pyruvate Decarboxylation Is A Limitation Of Kp-ipdc

In the no-induction fermentations, low levels of 2-ketoisovalerate were accumulated in the culture broth of *K. pneumoniae* Δ*budA*-Δ*ldhA-ipdC* (shown in Fig. 3). This indicated the decarboxylation reaction was still a limited step of the isobutanol synthesis pathway. However, a low level of isobutanol was obtained in the induced culture of *K. pneumoniae* Δ*budA*-Δ*ldhA-ipdC*. Furthermore, the 2-ketoisovalerate accumulated in the culture broth of *K. pneumoniae* Δ*budA*-Δ*ldhA-ipdC* was lower than that of *K. pneumoniae* Δ*budA*-Δ*ldhA-kivD*. We can conclude that the total carbon flux of the isobutanol synthesis pathway was more reduced in the IPTG induction conditions compared to the no-induction condition. High levels of ethanol and acetic acid were obtained in the culture broth of *K. pneumoniae* Δ*budA*-Δ*ldhA-ipdC* with IPTG induction, this indicated more pyruvate was converted to ethanol or acetic acid, instead of isobutanol synthesis.

Kp-IpdC and KivD are both ThDP-dependent decarboxylases. However, the substrate range of decarboxylases can be different with some classes, such as pyruvate decarboxylases, benzoylformate

decarboxylases and benzaldehyde lyases from bacteria or yeast accepting a broad variety of substrates, including keto acids and aldehydes [19]. The substrates of Ec-lpdC are limited to keto acids. The enzyme has the highest catalytic efficiency to the native substrate indole pyruvate (*Km* = 20 μM), to 4-Cl-benzoylformate and to 4-Br-benzoylformate. Pyruvate is also a substrate of this enzyme, but it has a very low affinity (*Km* = 3.38 mM) [32]. These data agree with the results obtained in this study, i.e., the *Km* of Kp-lpdC to pyruvate was found to be 3.31 mM (shown in Table 2).

Pyruvate conversion by Kp-lpdC is a disadvantage for isobutanol production. A high level of Kp-lpdC leads to more pyruvate being decarboxylated to aldehyde and reduces the available pyruvate for isobutanol synthesis. This finding explains the low titer of isobutanol caused by high expression of *ipdC* (see Fig. 1).

Protein Engineering To Improve The Substrate Specificity Of Kp-ipdc

Previously, different variants of decarboxylases have been constructed to alter substrate specificity. For example the I472 residue in the vicinity of the active centre of pyruvate decarboxylase (PDC) from *Zymomonas mobilis*. I472A enlarges the substrate binding site and allows the decarboxylation of longer aliphatic 2-keto acids (C4-C6) as well as aromatic 2-keto acids besides pyruvate [33]. Benzoylformate decarboxylase (BFD) from *Pseudomonas putida* favours aromatic 2-keto acids as substrate. The Ala460 residue in BFD is analogous to Ile472 in PDC. This alanine was replaced with isoleucine to obtain BFD A460I. The substrate binding site of BFD A460I was reduced and thus more similar of the wild type of PDC. BFD A460I can use pyruvate as the substrate, while the wild type of BFD is unable to convert it [34]. These successful examples demonstrate the application potential of decarboxylases and feasibility of changing their substrate specificities by point mutations.

For biosynthesis of the 6-carbon alcohol, 3-methyl-1-pentanol, engineering of KivD with the aim of achieving a higher selectivity toward 2-keto-4-methylhexanoate was performed. The F381L/V461A variant was the best one and produced 384.3 mg/L of 3-methyl-1-pentanol [35]. KivD was designed computationally to enhance its catalytic efficiency with C8 rather than C5 as a substrate. A triple-residues variant G402V/M538L/ F542V showed a 600-fold improvement in specificity for C8 compared to C5 substrates. But the enzyme activities with the two substrates were both decreased [36]. KivD introduced into *Synechocystis* results in two products, isobutanol and 3-methyl-1-butanol. To reduce the 3-methyl-1-butanol level and improve the isobutanol production many variants of KivD were constructed, and V461I/S286T showed the highest (2.4 times) improvement of the isobutanol to 3-methyl-1-butanol molar ratio [37]. Many protein engineering works were performed using decarboxylases, but the activities of variants with non-native substrates were still much lower than that using native substrates. *K*m of T290L and L546W of Kp-lpdC to 2-ketoisovalerate detected in this study were 1.17 mM and 1.01 mM. They are both higher than the *Km* of Ec-lpdC to its native substrate indole pyruvate (*K*m 20 μM) [32]. Isobutanol production by *K. pneumoniae* T290L was improved compared with *K. pneumoniae* lpdC. However,

isobutanol production by this strain with IPTG induction was still lower than that without IPTG induction, like that of *K. pneumoniae* lpdC. The pyruvate decarboxylation activity of T290L still effects isobutanol synthesis, and this disadvantage was not erased totally. Thus, there is still a large potential to improve the performance of Kp-lpdC.

Conclusion

5.5 g/L of isobutanol was produced by *K. pneumoniae* T290L in batch culture, which was 25% higher than that of the control strain. A substrate conversion ratio of 0.16 mol/mol was obtained. However, by-products of this strain still exhibited high levels and the isobutanol production is constrained by undesirable enzyme promiscuity of lpdC towards pyruvate. The protein engineering work showed promising results but there is scope for further improvement. One target could be to reduce the Km of Kp-lpdC to 2-ketoisovalerate to around 20 μM, near that of Ec-lpdC to indole pyruvate, in order to increase the efficiency of the biological route of isobutanol production further.

Declarations

Ethical Approval and Consent to participate

Not applicable.

Consent for publication

All authors have agreed that the manuscript should submit to Biotechnology for Biofuels.

Availability of data and material

The authors declare that the data supporting the findings of this study are available within the article and its supplementary information files.

Conflict of Interest

Authors declare that they have no conflict of interest.

Funding

This work was supported by National Key R&D Program of China (Grant No. 2019YFE0196900), Natural Science Foundation of Shanghai (Grant No. 19ZR1463600) , Royal Society-Newton Advanced Fellowship (Grant No. NAF\R2\180721).

Authors' contributions

Lin Shu: Investigation, Original draft preparation. Jinjie Gu: Investigation, Original draft preparation, Qinghui Wang: Investigation. Shaoqi Sun: Investigation. Youtian Cui: Software. Jason Fell: Software. Wai

Shun Mak: Software. Justin B. Siegel: Formal analysis. Jiping Shi: Formal analysis. Gary J. Lye: Formal analysis. Frank Baganz: Formal analysis, Writing - Review & Editing. Jian Hao: Conceptualization, Formal analysis. Writing - Review & Editing

Acknowledgments

FB would like to thank the Chinese Academy of Sciences for the award of a President's International Fellowship Initiative (Grant No. 2019VCB0007).

References

1. Machado IMP, Atsumi S: Cyanobacterial biofuel production. J Biotechnol. 2012, 162:50-56.
2. Reis CER, Rajendran A, Hu B: New technologies in value addition to the thin stillage from corn-to-ethanol process. Rev Environ Sci Biotechnol. 2017, 16:175-206.
3. Tao L, Tan EC, McCormick R, Zhang M, Aden A, He X, Zigler BT: Techno-economic analysis and life-cycle assessment of cellulosic isobutanol and comparison with cellulosic ethanol and n-butanol. Biofuel Bioprod Biorefin. 2014, 8:30-48.
4. Raju NP, Rao BA: Performance and Emission Characteristics of an Indirect Injection (IDI) Diesel Engine fuelled with Pongamia Methyl Ester (PME) and Isobutanol as an Additive. Int J Eng Res Technol. 2015, 4: 415-419.
5. Karabektas M, Hosoz M: Performance and emission characteristics of a diesel engine using isobutanol-diesel fuel blends. Renewable Energy. 2009, 34:1554-1559.
6. Ferreira MC, Meirelles AJA, Batista EAC: Study of the Fusel Oil Distillation Process. Ind Eng Chem Res. 2013, 52:2336-2351.
7. Generoso WC, Schadeweg V, Oreb M, Boles E: Metabolic engineering of *Saccharomyces cerevisiae* for production of butanol isomers. Curr Opin Biotechnol. 2015, 33:1-7.
8. Wess J, Brinek M, Boles E: Improving isobutanol production with the yeast *Saccharomyces cerevisiae* by successively blocking competing metabolic pathways as well as ethanol and glycerol formation. Biotechnol Biofuels. 2019, 12:173.
9. Atsumi S, Hanai T, Liao JC: Non-fermentative pathways for synthesis of branched-chain higher alcohols as biofuels. Nature. 2008, 451:86-89.
10. Atsumi S, Li Z, Liao JC: Acetolactate synthase from *Bacillus subtilis* serves as a 2-ketoisovalerate decarboxylase for isobutanol biosynthesis in *Escherichia coli*. Appl Environ Microbiol. 2009, 75:6306-6311.
11. Yu H, Wang N, Huo W, Zhang Y, Zhang W, Yang Y, Chen Z, Huo Y-X: Establishment of BmoR-based biosensor to screen isobutanol overproducer. Microb. Cell Factories. 2019, 18:30.
12. Hao J, Lin R, Zheng Z, Liu H, Liu D: Isolation and characterization of microorganisms able to produce 1, 3-propanediol under aerobic conditions. World J Microbiol Biotechnol. 2008, 24:1731-1740.

13. Chen C, Wei D, Shi J, Wang M, Hao J: Mechanism of 2, 3-butanediol stereoisomer formation in *Klebsiella pneumoniae*. App Microbiol Biotechnol. 2014, 98:4603-4613.
14. Wang D, Zhou J, Chen C, Wei D, Shi J, Jiang B, Liu P, Hao J: R-acetoin accumulation and dissimilation in *Klebsiella pneumoniae*. J Ind Microbiol Biotechnol. 2015, 42:1105-1115.
15. Wei D, Xu J, Sun J, Shi J, Hao J: 2-Ketogluconic acid production by *Klebsiella pneumoniae* CGMCC 1.6366. J Ind Microbiol Biotechnol. 2013:561-570.
16. Wang D, Wang C, Wei D, Shi J, Kim CH, Jiang B, Han Z, Hao J: Gluconic acid production by *gad* mutant of *Klebsiella pneumoniae*. World J Microbiol Biotechnol. 2016, 32:1-11.
17. Wang C, Wei D, Zhang Z, Wang D, Shi J, Kim CH, Jiang B, Han Z, Hao J: Production of xylonic acid by *Klebsiella pneumoniae*. App Microbiol Biotechnol. 2016, 100:10055-10063.
18. Gu J, Zhou J, Zhang Z, Kim CH, Jiang B, Shi J, Hao J: Isobutanol and 2-ketoisovalerate production by *Klebsiella pneumoniae* via a native pathway. Metab Eng. 2017, 43:71-84.
19. Pohl M, Sprenger GA, Müller M: A new perspective on thiamine catalysis. Curr Opin Biotechnol. 2004, 15:335-342.
20. Vogel C, Widmann M, Pohl M, Pleiss J: A standard numbering scheme for thiamine diphosphate-dependent decarboxylases. BMC Biochemistry. 2012, 13:24.
21. Andrews FH, McLeish MJ: Substrate specificity in thiamin diphosphate-dependent decarboxylases. Bioorg Chem. 2012, 43:26-36.
22. Kleiner D, Paul W, Merrick MJ: Construction of multicopy expression vectors for regulated over-production of proteins in *Klebsiella pneumoniae* and other enteric bacteria. J Gen Microbiol. 1988, 134:1779-1784.
23. Oh B-R, Heo S-Y, Lee S-M, Hong W-K, Park JM, Jung YR, Kim D-H, Sohn J-H, Seo J-W, Kim CH: Erratum to: Production of isobutanol from crude glycerol by a genetically-engineered *Klebsiella pneumoniae* strain. Biotechnol Lett. 2014, 36:397-402.
24. Song Y, DiMaio F, Wang Ray Y-R, Kim D, Miles C, Brunette TJ, Thompson J, Baker D: High-Resolution Comparative Modeling with RosettaCM. Structure, 2013, 21:1735-1742.
25. Bender BJ, Cisneros A, 3rd, Duran AM, Finn JA, Fu D, Lokits AD, Mueller BK, Sangha AK, Sauer MF, Sevy AM, et al: Protocols for Molecular Modeling with Rosetta3 and RosettaScripts. Biochemistry. 2016, 55:4748-4763.
26. Combs SA, DeLuca SL, DeLuca SH, Lemmon GH, Nannemann DP, Nguyen ED, Willis JR, Sheehan JH, Meiler J: Small-molecule ligand docking into comparative models with Rosetta. Nature Protocols. 2013, 8:1277-1298.
27. König S: Subunit structure, function and organisation of pyruvate decarboxylases from various organisms. Biochim Biophys Acta. 1998, 1385:271-286.
28. Smith KM, Cho K-M, Liao JC: Engineering *Corynebacterium glutamicum* for isobutanol production. App Microbiol Biotechnol. 2010, 87:1045-1055.

29. Higashide W, Li Y, Yang Y, Liao JC: Metabolic engineering of *Clostridium cellulolyticum* for production of isobutanol from cellulose. Appl Environ Microbiol. 2011, 77:2727-2733.
30. Miao R, Xie H, Lindblad P: Enhancement of photosynthetic isobutanol production in engineered cells of *Synechocystis* PCC 6803. Biotechnol Biofuels 2018, 11:267.
31. Acedos MG, Yustos P, Santos VE, Garcia-Ochoa F: Carbon flux distribution in the metabolism of *Shimwellia blattae* (p424IbPSO) for isobutanol production from glucose as function of oxygen availability. J Chem Technol Biotechnol. 2019, 94:850-858.
32. Schütz A, Golbik R, Tittmann K, Svergun DI, Koch MH, Hübner G, König S: Studies on structure-function relationships of indolepyruvate decarboxylase from *Enterobacter cloacae*, a key enzyme of the indole acetic acid pathway. Eur J Biochem. 2003, 270:2322-2331.
33. Pohl M, Siegert P, Mesch K, Bruhn H, Grötzinger J: Active site mutants of pyruvate decarboxylase from *Zymomonas mobilis*–a site-directed mutagenesis study of L112, I472, I476, E473, and N482. Eur J Biochem. 1998, 257:538-546.
34. Siegert P, McLeish MJ, Baumann M, Iding H, Kneen MM, Kenyon GL, Pohl M: Exchanging the substrate specificities of pyruvate decarboxylase from *Zymomonas mobilis* and benzoylformate decarboxylase from *Pseudomonas putida*. Protein Eng Des Sel. 2005, 18:345-357.
35. Zhang K, Sawaya MR, Eisenberg DS, Liao JC: Expanding metabolism for biosynthesis of nonnatural alcohols. Proc. Natl Acad Sci USA. 2008, 105:20653-20658.
36. Mak WS, Tran S, Marcheschi R, Bertolani S, Thompson J, Baker D, Liao JC, Siegel JB: Integrative genomic mining for enzyme function to enable engineering of a non-natural biosynthetic pathway. Nat Commun 2015, 6:10005.
37. Miao R, Xie H, F MH, Lindblad P: Protein engineering of α-ketoisovalerate decarboxylase for improved isobutanol production in *Synechocystis* PCC 6803. Metab Eng. 2018, 47:42-48.

Tables

Table 1
Strains and plasmids

Strains or plasmids	Relevant genotype and description	Reference
K. pneumoniae strains		
CGMCC 1.6366	TUAC01 Wild type	[12]
Δ*budA*-Δ*ldhA -ipdC*	Δ*budA*, Δ*ldhA*, pDK6-*ipdC*	This work
Δ*budA*-Δ*ldhA -kivD*	Δ*budA*, Δ*ldhA*, pDK6-*kivD*	This work
IpdC	Δ*budA*, Δ*ldhA*, Δ*ipdC*, pDK6-*ipdC*	[18]
KivD	Δ*budA*, Δ*ldhA*, Δ*ipdC*, pDK6-*kivD*	This work
T290L	Δ*budA*, Δ*ldhA*, Δ*ipdC*, pDK6-*ipdC-T290L*	This work
L546W	Δ*budA*, Δ*ldhA*, Δ*ipdC*, pDK6-*ipdC-L546W*	This work
E. coli strains		
E. coli DH5a	Host of plasmid	Lab stock
BL21(DE3)	Host of plasmid	Lab stock
BL21/*ipdC*	Carries pET28a-*ipdC*	This work
BL21/*kivD*	Carries pET28a-*kivD*	This work
BL21/D289L	Carries pET28a-*ipdC*-D289L	This work
BL21/T290L	Carries pET28a-*ipdC*-T290L	This work
BL21/Q383M	Carries pET28a-*ipdC*-Q383M	This work
BL21/A387I	Carries pET28a-*ipdC*-A387I	This work
BL21/F388W	Carries pET28a-*ipdC*-F388W	This work
BL21/A387L	Carries pET28a-*ipdC*-A387L	This work
BL21/V542I	Carries pET28a-*ipdC*-V542I	This work
BL21/L546W	Carries pET28a-*ipdC*-L546W	This work
BL21/D289L+T290L	Carries pET28a-*ipdC*-D289L+T290L	This work
BL21/A387I+F388W	Carries pET28a-*ipdC*-A387I+F388W	This work
Plasmids		
pDK6	Kan^r, lacIQ, tac, 5.1 kb	[22]
pDK6-*kivD*	pDK6 carries *kivD*	[18]

Strains or plasmids	Relevant genotype and description	Reference
pDK6-*ipdC*	pDK6 carries *ipdC*	[18]
pET28a	vector carries N-terminal His Tag, Kan^r, 5,369 bp	Novagen®
pGEM-*kivD*	Vector holding *kivD* (*L. lactis*)	[23]
pMD18-T-*ipdC*	Amp^r, carries *ipdC*,	[18]
pET28a-*kivD*	pET28a carries *kivD*	This work
pET28a-*ipdC*	pET28a carries *ipdC*	This work

Table 2
Kinetic parameters 2-ketoisovalerate and pyruvate decarboxylation catalyzed by Kp-lpdC or KivD

Substrate	Enzyme	*K*m (mM)	Vmax (mM/min)	*K*cat (s^{-1})	*K*cat/*K*m ($M^{-1}s^{-1}$)
2-Ketoisovalerate	Kp-lpdC	1.48	0.037	8.05	5445.39
	KivD	4.18	0.0409	3.46	828.31
Pyruvate	Kp-lpdC	3.13	0.0115	0.58	183.70
	KivD	18.81	0.0034	0.28	15.09

Table 3
Kinetic parameters of variants of Kp-lpdC with 2-ketoisovalerate or pyruvate as substrates.

Variants	Substrate	*K*m (mM)	Vmax (mM/min)	*K*cat (s^{-1})	*K*cat/*K*m ($M^{-1}s^{-1}$)
Kp-lpdC	2-Ketoisovalerate	1.48	0.037	8.05	5445.39
	Pyruvate	3.13	0.0115	0.58	183.70
A387L	2-Ketoisovalerate	5.91	0.0024	0.31	52.57
	Pyruvate	13.19	0.0024	0.21	15.63
F388W	2-Ketoisovalerate	16.77	0.02	2.9	172.68
	Pyruvate	n.d.	n.d.	n.d.	n.d.
V542I	2-Ketoisovalerate	1.99	0.018	2.88	1443.98
	Pyruvate	23.38	0.0056	0.9	38.39
L546W	2-Ketoisovalerate	1.01	0.034	2.59	2559.61
	Pyruvate	693.27	0.085	6.66	9.61
D289L+T290L	2-Ketoisovalerate	n.d.	n.d.	n.d.	n.d.
	Pyruvate	n.d.	n.d.	n.d.	n.d.
A387I+F388W	2-Ketoisovalerate	48.07	0.017	0.704	14.653
	Pyruvate	n.d.	n.d.	n.d.	n.d.
D289L	2-Ketoisovalerate	n.d.	n.d.	n.d.	n.d.
	Pyruvate	n.d.	n.d.	n.d.	n.d.
T290L	2-Ketoisovalerate	1.17	0.0383	2.97	2609.8
	Pyruvate	11.272	0.0059	0.46	40.5
Q383M	2-Ketoisovalerate	1.88	0.03	4.18	2215.2
	Pyruvate	19.7	0.016	2.16	109.4
A387I	2-Ketoisovalerate	23.4	0.034	1.61	68.62

Variants	Substrate	*K*m (mM)	Vmax (mM/min)	*K*cat (s^{-1})	*K*cat/*K*m ($M^{-1}s^{-1}$)
	Pyruvate	39.7	0.0051	0.24	6.02

Figures

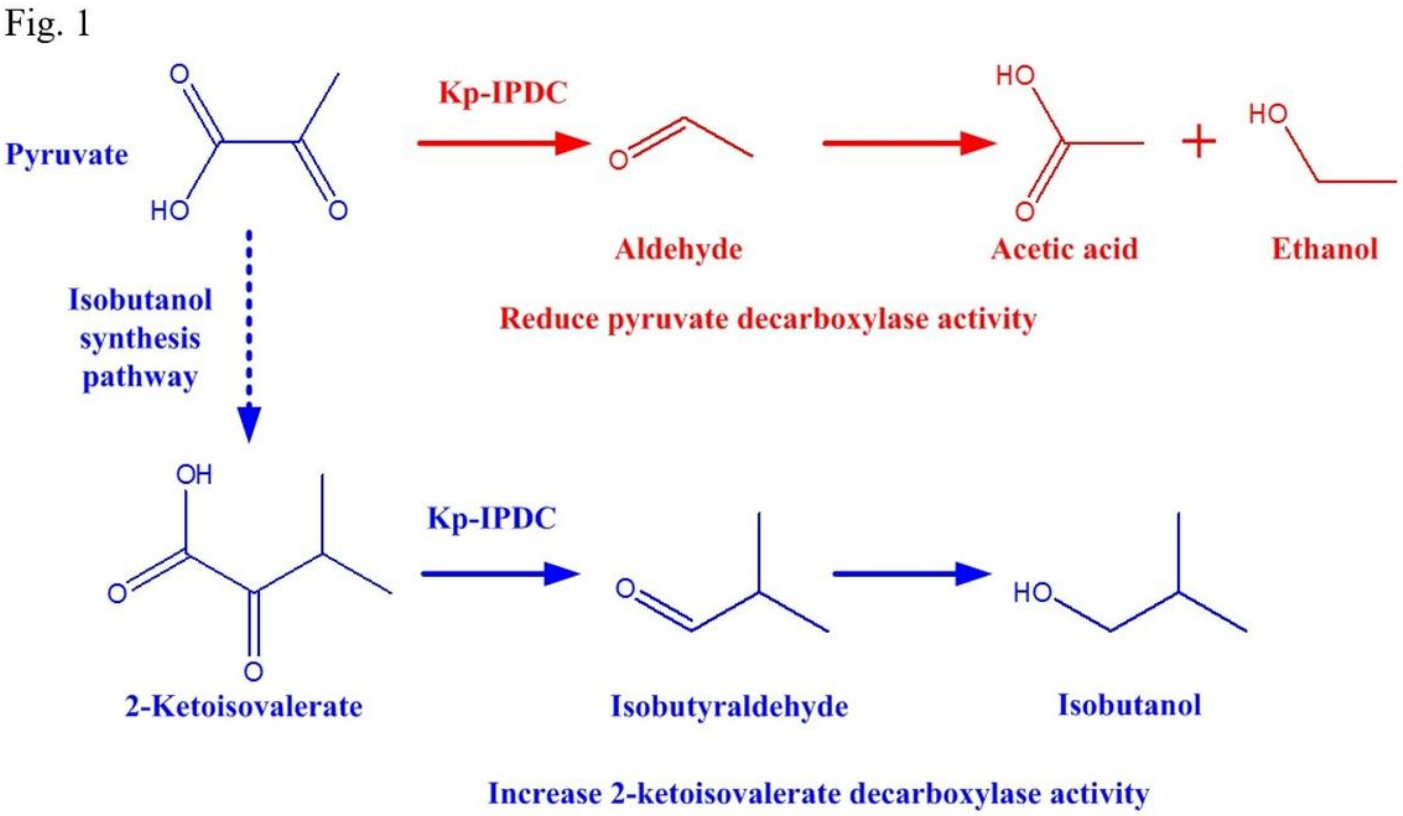

Figure 1

Metabolic pathway of isobutanol synthesis and branch pathway in K. pneumoniae. Kp-IpdC is catalysing the 2-ketoisovalerate decarboxylation and further conversion to isobutanol (blue route). It was suspected that the pyruvate decarboxylase activity of Kp-IpdC reduced the available pyruvate for isobutanol synthesis (red route).

Fig.2

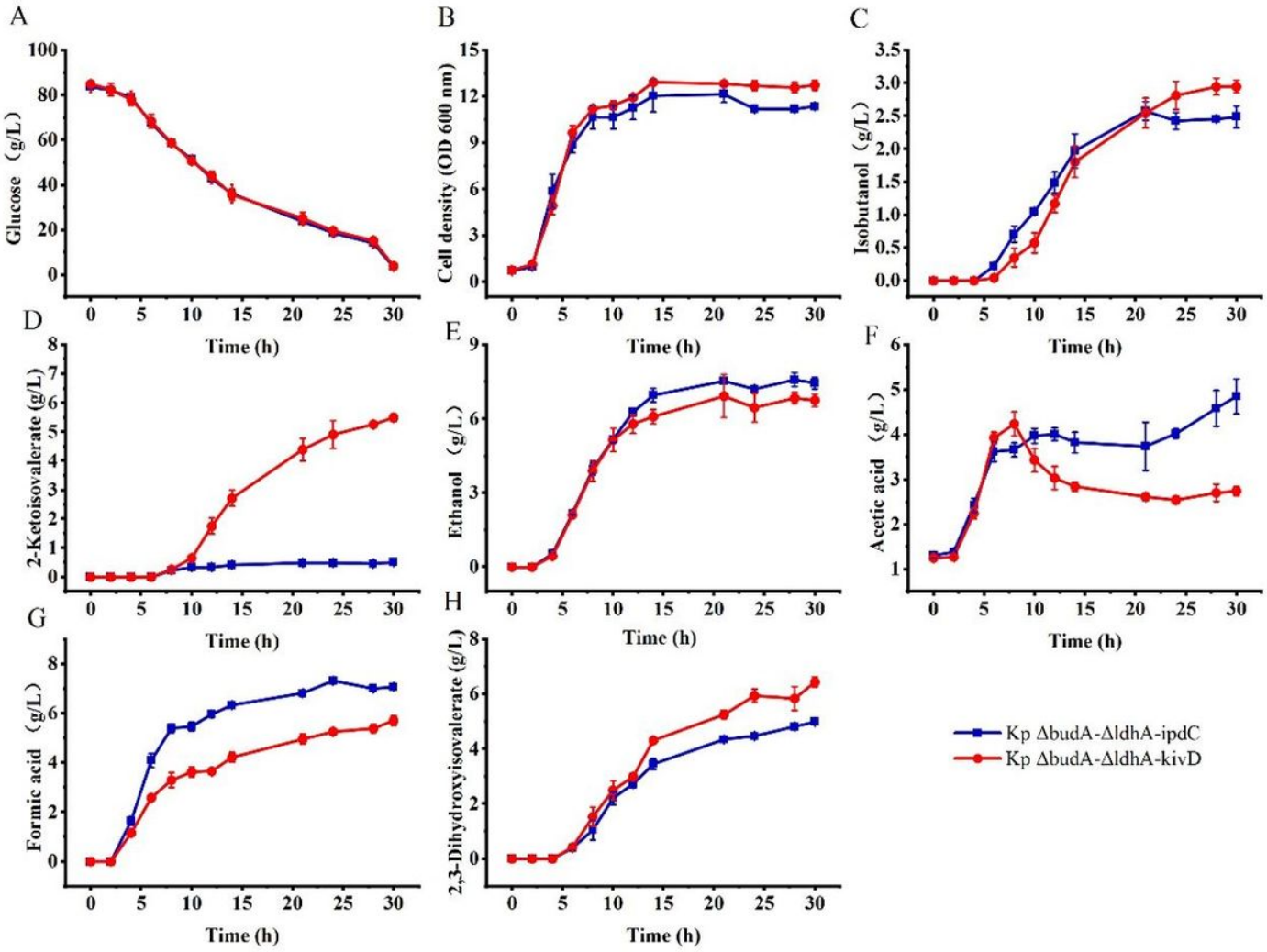

Figure 2

The cell growth and metabolite production of K. pneumoniae ΔbudA-ΔldhA-ipdC and K. pneumoniae ΔbudA-ΔldhA-kivD in the batch culture with IPTG induction. Cells were cultured in 5 L bioreactors and 1 mM of IPTG was added to the culture broth after 8 hours of cultivation. Data points are the average of n = 3; error bars represent standard error about the mean.

Fig. 3

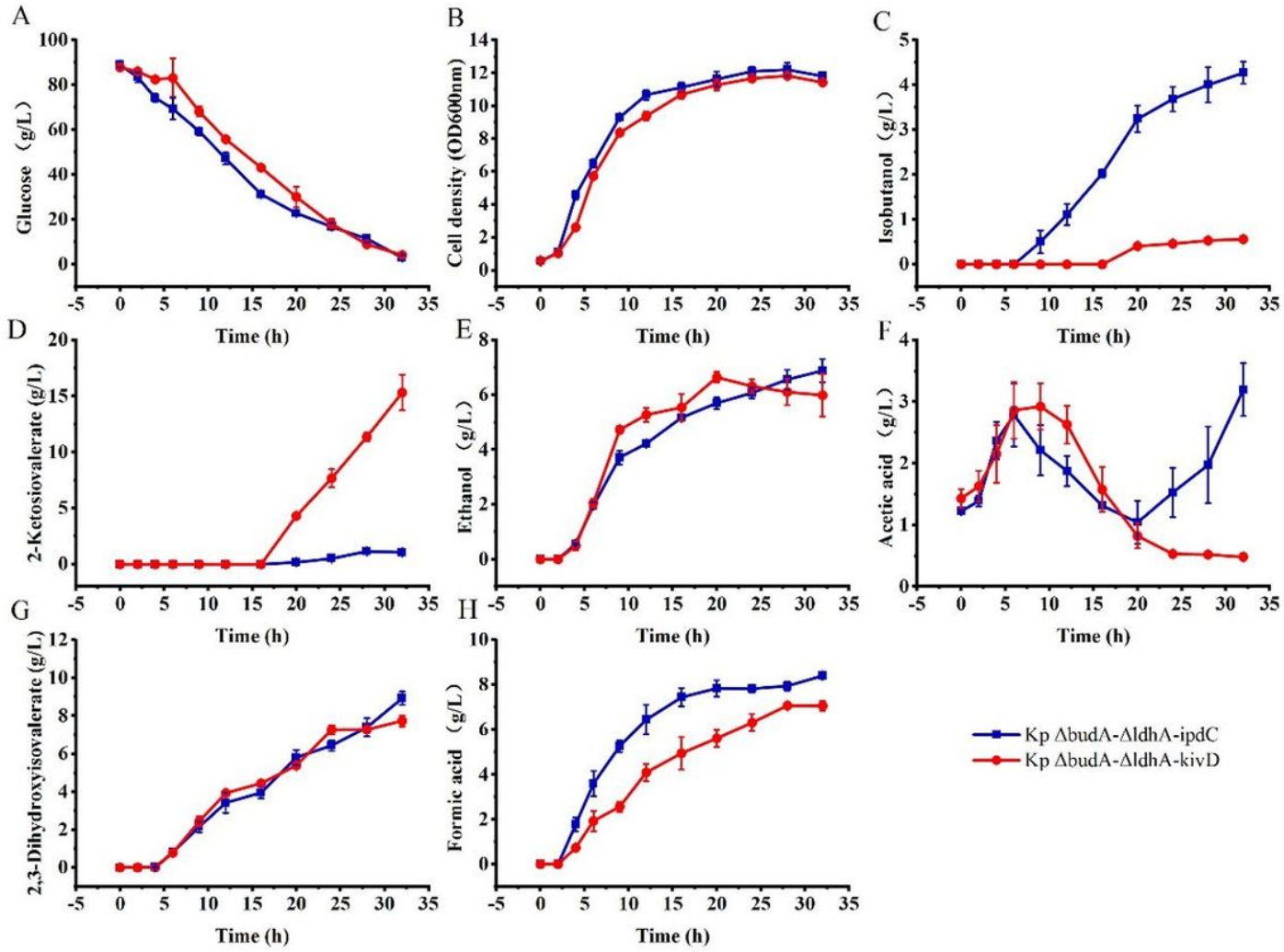

Figure 3

The cell growth and metabolite production of K. pneumoniae ΔbudA-ΔldhA -ipdC and K. pneumoniae ΔbudA-ΔldhA-kivD in the batch culture without IPTG induction. Cells were cultured in 5 L bioreactors and no IPTG was added to the culture broth in the process. Data points are the average of n = 3; error bars represent standard error about the mean.

Fig .4

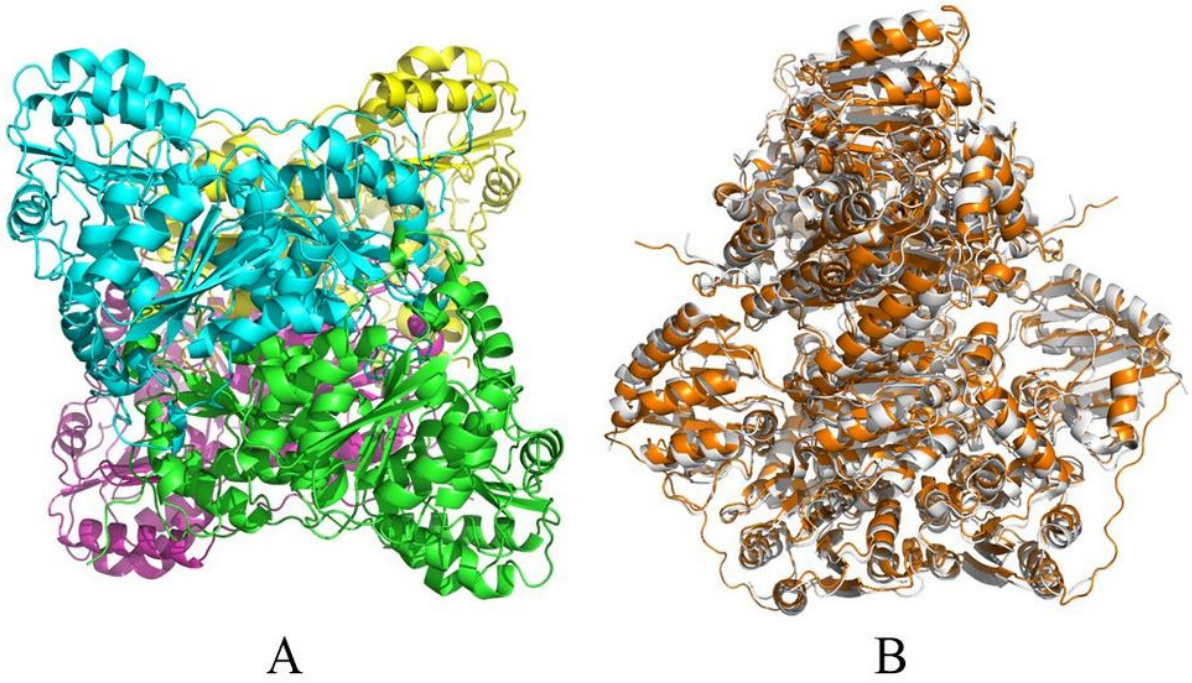

Figure 4

A: the predicted tetrameric structure of Kp-lpdC; B: Structural overlay of Kp-lpdC (orange) with Ec-lpdC (gray). The Root Mean Square Deviation (RMSD) of Kp-lpdC and Ec-lpdC monomers was 1.158

Fig. 5

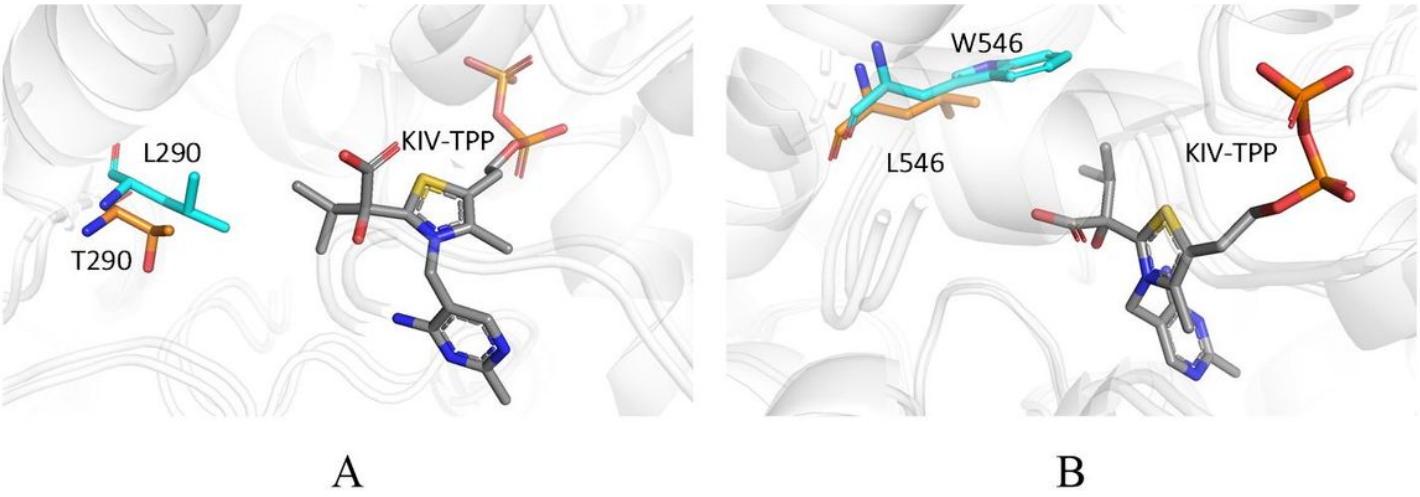

Figure 5

3D structure of the active centre of Kp-IpdC with substrate bound obtained from simulations using PyMOL. A: T290L. B: L546W.

Fig. 6

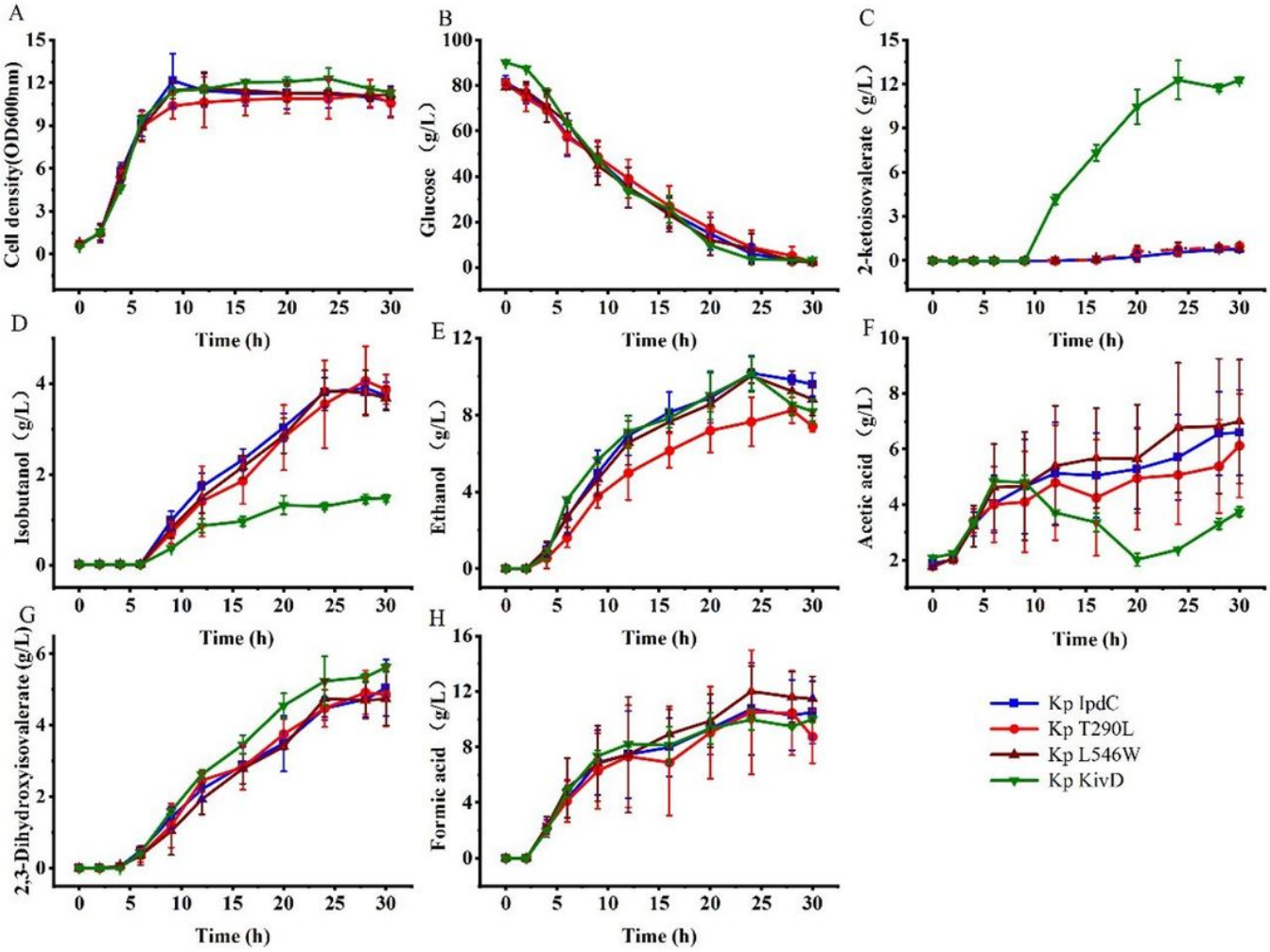

Figure 6

The cell growth and metabolites production of K. pneumoniae IpdC, K. pneumoniae T290L, K. pneumoniae L546W, and K. pneumoniae KivD in the batch cultures with IPTG induction. Cells were cultured in 5 L bioreactors and 1 mM of IPTG was added to the culture broth after 8 hours of cultivation. Data points are the average of n = 3; error bars represent standard error about the mean.

Fig. 7

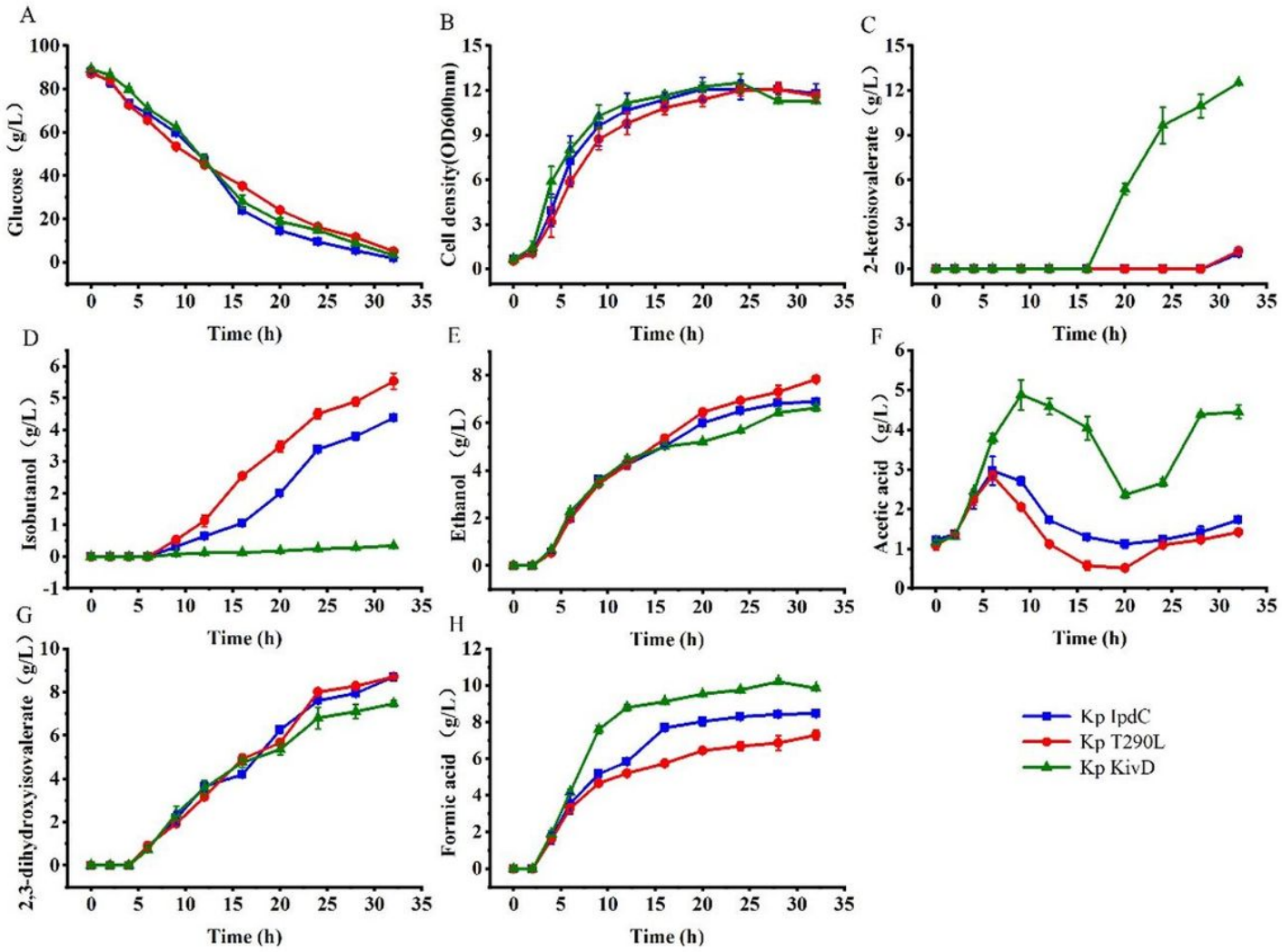

Figure 7

The cell growth and metabolites production of K. pneumoniae IpdC, K. pneumoniae T290L, and K. pneumoniae KivD in the batch cultures without IPTG induction. Cells were cultured in 5 L bioreactors and no IPTG was added to the culture broth in the process. Data points are the average of n = 3; error bars represent standard error about the mean.

Supplementary Files

This is a list of supplementary files associated with this preprint. Click to download.

- Supplementary1204.docx